Three-dimensional axisymmetric flow-focusing device using stereolithography

Yuya Morimoto · Wei-Heong Tan · Shoji Takeuchi

Abstract This paper describes a three-dimensional microfluidic axisymmetric flow-focusing device (AFFD) fabricated using stereolithography. Using this method, we can fabricate AFFDs rapidly and automatically without cumbersome alignment needed in conventional methods. The AFFDs are able to be fabricated reproducibly with a micro-sized orifice of diameter around 250 μm. Using this device, we are able to produce monodisperse water-in-oil (W/O) droplets with a coefficient of variation (CV) of less than 4.5%, W/O droplets with encapsulated microbes (CV< 4.9%) and oil-in-water (O/W) droplets (CV<3.2%) without any surface modifications. The diameter of these droplets range from 54 to 244 μm with respect to the flow rate ratio of the fluids used; these results are in good agreement with theoretical behavior. For applications of the AFFD, we demonstrate that these devices can be used to produce double emulsions and monodisperse hydrogel beads.

Y. Morimoto · W.-H. Tan · S. Takeuchi (✉)
Center for International Research on MicroMechatronics
(CIRMM), Institute of Industrial Science (IIS),
The University of Tokyo,
4-6-1 Komaba,
Meguro-ku, Tokyo 153-8505, Japan
e-mail: takeuchi@iis.u-tokyo.ac.jp

S. Takeuchi
PRESTO, Japan Science and Technology Agency,
Chiyoda-ku, Tokyo 102-0075, Japan

1 Introduction

Highly monodisperse hydrogel microbeads have many important applications in pharmacy (Nortier et al. 1995), food coatings (Sanguansri et al. 2006) and biomedical industries such as cell encapsulation (Jen et al. 1996; Luca et al. 2007) and drug delivery systems (Graham and Mcneill 1984). In cell encapsulation for tissue engineering and cell-based beads array systems, micro-sized monodisperse hydrogel beads are in demand since they facilitate handling and allow rapid exchange of nutrients into and waste out of these beads. Many groups have demonstrated the production of monodisperse hydrogel beads from monodisperse droplets (Tan and Takeuchi 2007; Kim et al. 2007; Zhang et al. 2007; Shintaku et al. 2007; Sugiura et al. 2005; Choi et al. 2007). To produce monodisperse droplets, quasi-two-dimensional (2D) planar microfluidic devices, such as T-junction microchannels (Nisisako et al. 2002) and 2D microfluidic flow-focusing devices (Anna et al. 2003; Garstecki et al. 2004), are often used. In these devices, the type of dispersion that can be produced is dictated by the surface chemistry of the channel walls, i.e. hydrophobicity or hydrophilicity. Channels exhibiting hydrophobicity are suitable for dispersing water-in-oil (W/O) droplets whereas those exhibiting hydrophilicity are suited for oil-in-water (O/W) dispersions. The problem of wetting occurs when hydrophobic channels are used to produce O/W dispersions and vice versa, thereby restricting the kinds of emulsions that can be produced in such devices. In some cases, fouling of channel surfaces by proteins and carbohydrates might make the formation of even W/O dispersions in hydrophobic channels difficult (Tan and Takeuchi 2007). In order to circumvent this problem, it is necessary to modify the surface of 2D microfluidic channels (e.g., silanization) to cater for each usage (Okushima et al. 2004).

The use of a microfluidic three-dimensional (3D) axisymmetric flow-focusing device (AFFD) proved to be effective in forming monodisperse emulsions without wetting (Takeuchi et al. 2005; Utada et al. 2007). In the AFFD, we avoid the wetting problem as the inner fluid is surrounded by the outer fluid and does not contact the channel walls (Fig. 1(a)). Nevertheless, the use of AFFDs are still rather limited as conventional methods to fabricate AFFDs are non-reproducible, suffer from low yield as they are handmade, and are unsuitable for mass production. To solve this problem, several groups have suggested fabricating AFFDs with micro electro mechanical systems (MEMS) techniques (Huang et al. 2006; Luque et al. 2007). Although we can produce AFFDs accurately using MEMS techniques, the fabrication process is tedious and the device requires additional packaging such as the attachment of Teflon adaptors and gluing of tubes for external connections. Therefore, we think that AFFDs fabricated by MEMS techniques are inconvenient to use and are not appropriate tools for mass production of monodisperse emulsions.

Here, we propose the fabrication of AFFDs with stereolithography. Stereolithography is a rapid and automatic process for producing complicated three-dimensional objects (Zhang et al. 1999; Zissi et al. 1996). Advantages of AFFDs fabricated using stereolithography over conventional methods are: (a) ability to produce seamless channels with precise alignment that does not leak even at high flow rates, (b) suitability for large scale production due to the automated fabrication process, and (c) easy integration of 3D features such as microfluidic channels and inlet/outlet ports that allows convenient external connections. In this paper, we have formed a micro-sized axisymmetric channel inside our AFFD with high alignment accuracy. The device allowed us to form monodisperse micro-sized emulsions and hydrogel beads regardless of the combination of fluids used. In addition, we realized complicated designs (e.g., connection ports, axisymmetric flow channels) that are not possible in conventional devices made with photolithographic methods using poly(dimethylsiloxane) (PDMS) holes for tubing (Tan and Takeuchi 2007; Takeuchi et al. 2005; Huang et al. 2006) Features such as connection ports greatly reduced leakage failures due to poor adhesion of adaptor ports and allowed experiments to be performed with minimal fuss and preparation.

2 Experiment procedure and physical background

2.1 Design and fabrication of AFFD

Figure 1(b) shows the design of our AFFD to produce monodisperse droplets and hydrogel beads. The device
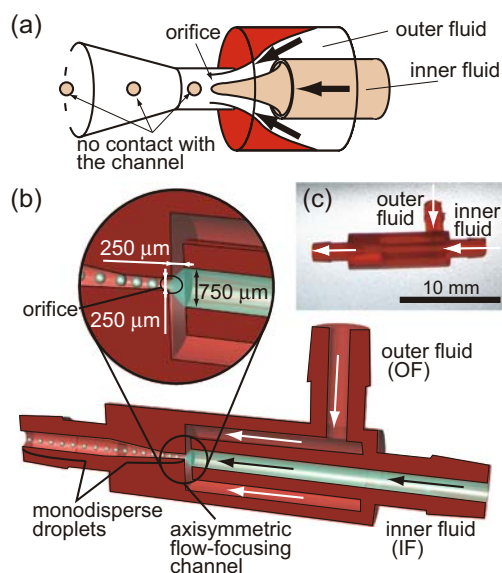

Fig. 1 (a) The inner fluid is focused and broken into droplets at the orifice of an AFFD. No wetting occurs since droplets are shielded from the channel walls, allowing monodisperse emulsions to be produced regardless of the kind of the fluids used. (b) Cross-sectional view of our AFFD fabricated using stereolithography to produce monodisperse droplets. The AFFD has an axisymmetric flow-focusing channel and connection ports which cannot be realized by conventional MEMS techniques. (c) The photo of the actual AFFD

consists of two concentric hollow cylinders. Each cylinder has a connection port that separately guides a fluid into the device (see the Supplementary 1). These fluids are immiscible and when they are focused at the axisymmetric flow-focusing orifice, the inner fluid breaks up into droplets. By varying the flow rate ratio of the inner fluid and the outer fluid, the size of droplets can be controlled. The inner fluid is always surrounded by the outer fluid and the droplets formed are confined to the central axis of the microchannel. As they do not contact the channel surface, AFFDs avoid the problem of wetting even when various kinds of droplets are produced.

Figure 1(c) shows the photo of our AFFD, it consists of three connection ports (two inlets and one outlet) and measures 18.55 mm in length. We designed this device with 3D modeling software (Rhinoceros, AppliCraft) and used a commercial stereolithography modeling machine (Perfactory, Envision Tec, Germany) to fabricate the AFFD. Light is projected plane-by-plane by a digital micromirror device (DMD) projector into a reservoir of photosensitive acrylates resin ("R11, 25–50 μm layers", Envision Tec) that consists of acrylic oligomer, dipentaerythritol pentaacrylate, propoxylated trimethylolpropane triacrylate, photoinitiator and stabilizers. The resin crosslinks and cures when exposed, and complicated 3D structures are realized by prototyping layer by layer while the base plate gradually moves up (Fig. 2(a)). Each projected
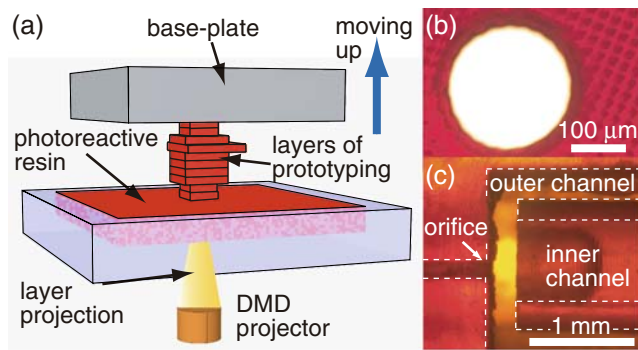
Fig. 2 (**a**) Fabrication principles: DMD projector casts a light to cure the photoreactive resin layer-by-layer. After each exposure, the base plate moves up 50 μm. Photos showing (**b**) the circular orifice measuring 255 μm in diameter and (**c**) the cross-section of the axisymmetric flow-focusing channel

plane has an area of 10.5×14 mm^2 and measures 50 μm in thickness. The spatial resolution of this technique is 16 μm in the horizontal (x, y) directions and 50 μm in the vertical (z) direction. The production rate in the z direction is 2.5 mm/h, and it takes about 8 h to fabricate six AFFDs simultaneously in a single run.

Figure 2(b) shows the close-up of the orifice measuring 255 μm in diameter that is fabricated using stereolithography. We fabricated only the axisymmetric channel portion of the device using stereolithography and measured the diameters of 12 such samples. The designed diameter was 250 μm and the measured average diameter was 254 μm (249–259 μm). The smallest orifice that can be fabricated with our stereolithography equipment is around 150 μm in diameter, but these small orifices were not as reproducible as those with diameters around 250 μm. Thus, the AFFD with 254 μm orifices was used in all our experiments. Also, we can see from the cross-section of the device (Fig. 2(c)) that the orifice and the inner channel were positioned axisymmetrically, indicating that stereolithography can produce complicated features reproducibly and accurately. To investigate the fabrication accuracy of stereolithography, we measured the roughness of a block fabricated by stereolithography using a Dectak profilometer (Dectak 6M, ULVAC, Inc.) (see the Supplementary 2). The roughness average (Ra) of the block is 916 nm and the average misalignment between each layer is 213 nm. Also, the height difference between the peak and valley for a length 1.5 mm is less than 4 μm. In addition, our devices allow us to work with a greater repertoire of organic solvents compared to conventional PDMS devices; our devices fabricated by stereolithography were immersed in hexadecane and 2-propanol for more than 6 h and there was no observable damage to our devices although these organic solvents are known to swell PDMS quickly and seriously degrade device performance.

2.2 Materials

We used sodium alginate (80–120 mPa · S), corn oil and lecithin (soybean), soybean oil (Wako Pure Chemical Industries, Ltd.), hexadecane, Tween 20, Span 80 (Kanto Chemical Co., Inc.), acetic acid (Nacalai Tesque, Inc.) and low melting point agarose (Agarose, Type IX-A, glass transition temperature (T_g)=17°C at 1.5%, SIGMA-Aldrich). Calcium carbonate (CaCO$_3$) nano-particles (NPCC-Fresh slurry, 8.0 wt.% Slurry) were kindly supplied by Nano-Materials Technology Pte Ltd (Singapore). Other chemicals were purchased from Kanto Chemical Co., Inc., Nacalai Tesque and Wako Pure Chemical Industries. *Washing buffer* for separating alginate gel beads from corn oil consists of CaCl$_2$ (81 mM), KCl (1.34 mM), phenol red (0.02 mM) and Tween 20 (1 wt.%). Tris–acetate–phosphate (TAP) buffer consists of NH$_4$Cl (7.48 mM), MgSO$_4$ (406 μM), CaCl$_2$ (340 μM), K$_2$HPO$_4$ (540 μM), KH$_2$PO$_4$ (463 μM), H$_3$BO$_3$ (184 μM), ZnSO$_4$ (76.5 μM), MnCl$_2$ (25.5 μM), FeSO$_4$ (17.9 μM), CoCl$_2$ (6.77 μM), (NH$_4$)$_6$Mo$_7$O$_{24}$ (0.88 μM), CuSO$_4$ (6.29 μM) and Na$_2$EDTA (148 μM). Unless otherwise specified, all water used in the experiments refers to ultra pure water obtained from a Millipore system having a specific resistance of 18 MΩ · cm.

2.3 Experimental procedures

The droplet size is affected by the orientation of the AFFD (Takeuchi et al. 2005). Here, we oriented the device vertically for all the experiments (Fig. 3(a)). Tefzel® tubes were attached to the inlet and outlet ports using silicone rubber tubes and we infused inner and outer fluids into the device through these tubes using syringe pumps (KDS-210, KD Scientific Inc., USA). We allowed the system to stabilize for 2 min before emulsions and hydrogel beads were collected for measurements of their diameters using a digital microscope (VHX-900, KEYENCE Co.). *Chlamydomonas* (*Chlamydomonas reinhardtii* wild type +), a unicellular flagellate, was used for cell encapsulation experiments. Synchronous cultures of *Chlamydomonas* were incubated for 3 days in TAP buffer using a 14/10-h light/dark cycle while air was bubbled continuously into the TAP buffer to supply O$_2$ and to stir the cells.

Figure 3(b) and (c) shows the schematic diagrams for the formation of monodisperse alginate and agarose hydrogel beads, respectively. For producing alginate gel beads, we used the internal gelation method (Poncelet 2001) (Fig. 3(b)). Corn oil with lecithin (2 wt.%) and Na-alginate solution (1 wt.%) containing insoluble CaCO$_3$ nano-particles (37.5 mM) were used for the outer and the inner fluids, respectively. Farther downstream, acetic acid dissolved in corn oil with lecithin (75 mM) was introduced into the main stream. As acetic acid dissolves in both polar and non-polar
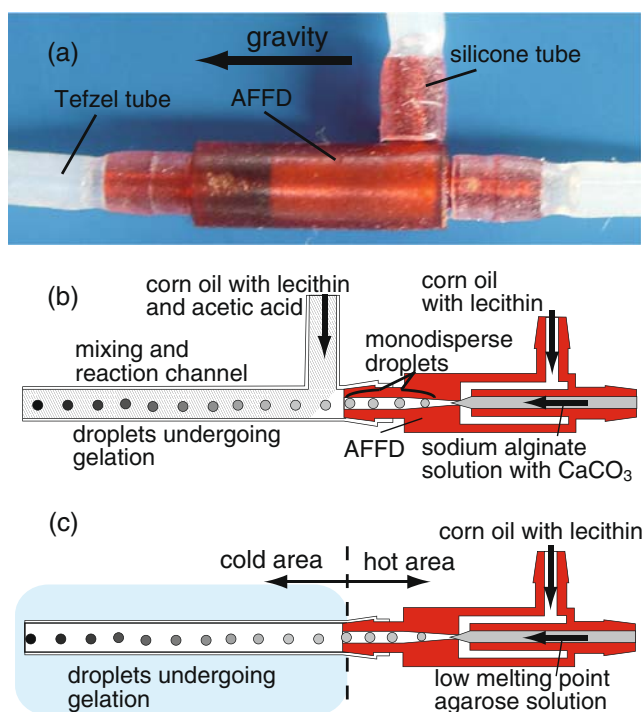
Fig. 3 (a) Photo of the experimental setup. Tefzel tubes and silicone tubes were attached to the inlets and outlet of the vertically mounted AFFD. Schematic diagrams showing (b) alginate gel formation by internal gelation. pH reduction in droplets caused by acetic acid induce gelation. (c) Agarose gel formation. Agarose gel beads are formed by cooling down agarose droplets to below its T_g

solvents, it gradually diffuses into the alginate droplets after being introduced into the main stream. A pH decrease in the alginate droplets releases Ca^{2+} ions from insoluble $CaCO_3$ nano-particles which react with Na-alginate to form Ca-alginate gel.

For producing agarose gel beads, we used corn oil with lecithin and low melting point agarose solution (1.5 wt.%) as the outer and inner fluids, respectively (Fig. 3(c)). This setup consisted of (a) a hot area where the syringe containing agarose solution was heated to 50°C by a syringe heater (SWS-10, Warner Instruments) and the AFFD to 60°C by a heater (ThermoPlate, TOKAI HIT CO., LTD), and (b) a cold area which was controlled using ice water (0°C). Monodisperse droplets of low melting point agarose solution were formed in the hot area and solidified when the emulsion cooled down below the T_g of the low melting point agarose in the cold area.

Hydrogel beads were suspended in corn oil when we collected them from the AFFD. Detail procedures on the transferring of hydrogel beads to water from corn oil are reported in another paper (Tan and Takeuchi 2007). Briefly, we first collected these beads in a microtube including corn oil with lecithin. When the hydrogel beads settled down after 5 min, we aspirated off the excess oil. Subsequently, we added hexane to dissolve the residual corn oil and

resuspended the beads in hexane. Hexane was added because it is easier to extract the beads from hexane than from corn oil, and we found that there was lower occurrence of bead aggregation when hexane was used. We again aspirated off excess hexane after the beads settled down, and carefully added *washing buffer* or Tween 20 solution (1 wt.%) to separate alginate gel beads and agarose gel beads from the oil, respectively. After the hydrogel beads were suspended in the *washing buffer* or Tween 20 solution, we collected these beads by centrifugation. We aspirated off the supernatant and resuspended these beads in water. Several cycles of centrifuging, disposal of the supernatant and resuspending in water were repeated for rinsing.

2.4 Physical background

Figure 4 shows the general structure of the axisymmetric channel in an AFFD. The outer fluid focuses the inner fluid into a jet stream when both fluids flow through the orifice (Martin-Banderas et al. 2006). After this jet stream goes out of the orifice, it is broken into droplets. This phenomenon is classified into two types; namely, dripping and jetting (Utada et al. 2005, Ambravaneswaran et al. 2004). The type of drop formation depends on the capillary number of the interface between the inner and outer fluid

$$Ca = \frac{\eta_{of} v}{\gamma} = \frac{\eta_{of} Q_{IF}}{\pi \gamma R_{jet}^2} \qquad (1)$$

where Ca is the capillary number, η_{of} is the viscosity of the outer fluid, Q_{IF} is the flow rate of the inner fluid, γ is the interfacial tension, R_{jet} is the radius of the inner jet stream and v is the downstream velocity of the inner fluid. When Ca<1, interfacial forces dominate over inertial forces. In this case, droplets are formed close to the exit of the orifice, leading to dripping. When inertial forces dominate, i.e. Ca> 1, and the jet grows faster than the forming of droplets and consequently droplets are formed downstream, leading to
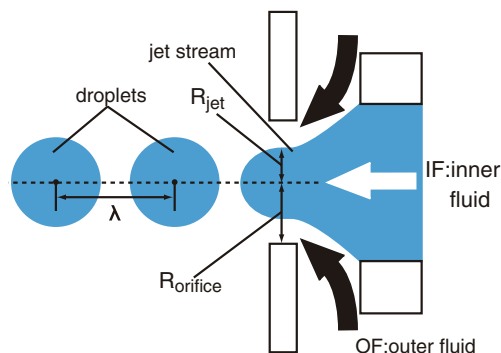

Fig. 4 General structure of the axisymmetric flow-focusing channel. The inner and outer fluids focus at the orifice to become coaxial jet streams. When the jet stream of the inner fluid comes out of the orifice, it breaks up into droplets

jetting. The droplets produced by jetting are more poly-disperse and larger than those produced by dripping. Therefore, we want to operate in the dripping range in order to produce monodisperse droplets.

In the dripping condition, droplets are formed near the exit of the orifice and the flow rate ratio can be expressed as a function of cross-sectional area. For this relationship, we can calculate the radius of the jet stream as follows,

$$\frac{Q_{\mathrm{IF}}}{Q_{\mathrm{OF}}} = \frac{\pi R_{\mathrm{jet}}^2}{\pi R_{\mathrm{orifice}}^2 - \pi R_{\mathrm{jet}}^2}$$

or,

$$R_{\mathrm{jet}}^2 = \frac{R_{\mathrm{orifice}}^2}{\frac{Q_{\mathrm{OF}}}{Q_{\mathrm{IF}}} + 1} \quad (2)$$

where Q_{OF} is the flow rate of the outer fluid and R_{orifice} is the orifice radius. When the droplets are produced at equal intervals, the volume of a droplet is expressed by the relation between the cross-sectional area of the inner jet stream and the droplet interval, i.e.,

$$\lambda = \frac{\frac{4}{3} R_{\mathrm{drop}}^3}{R_{\mathrm{jet}}^2} \quad (3)$$

where R_{drop} is the radius of droplets and λ is the droplet interval. In addition, Tomotika (Tomotika 1935) found that the droplet interval is also proportional to the radius of the droplets:

$$\lambda = k R_{\mathrm{drop}} \quad (4)$$

where k is the constant of proportion determined by the viscosity ratio of the inner fluid to the outer fluid. Therefore, we are able to predict the droplet radius by combining both relationships to give:

$$R_{\mathrm{drop}} = C \frac{R_{\mathrm{orifice}}}{\sqrt{\frac{Q_{\mathrm{OF}}}{Q_{\mathrm{IF}}} + 1}} \quad (5)$$

where C is a constant value depending on the properties of the fluids used. Droplet radius is proportional to $\left(\frac{Q_{OF}}{Q_{IF}} + 1\right)^{-\frac{1}{2}}$ when we use the same device and the same fluids in the inner and the outer fluid. This relationship indicates that with the AFFD we are able to change the size of droplets by controlling the flow rate ratio.

3 Results and discussion

3.1 Formation of monodisperse droplets

We used the AFFD to demonstrate the formation of monodisperse W/O droplets with various combinations of inner/outer fluids. Figure 5(a) and (b) shows images of W/O
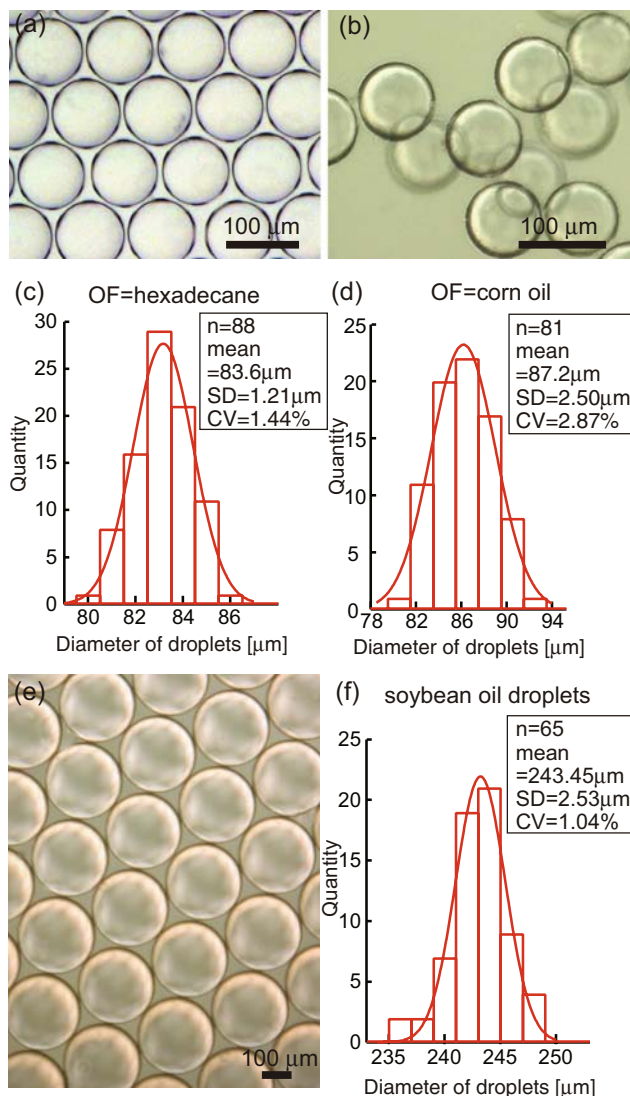

Fig. 5 Images of monodisperse water droplets in (**a**) hexadecane and (**b**) corn oil produced by the AFFD. For (**a**) and (**b**): $Q_{\mathrm{OF}}/Q_{\mathrm{IF}}$ is 37.5 (Q_{IF}=12 µl/min). (**c**) and (**d**) Diameter distribution of water droplets shown in (**a**) and (**b**), respectively. (SD is standard deviation and CV is coefficient of variation.) (**e**) Image of soybean oil droplets. The outer fluid is water with Tween 20 (1.5 wt.%) and the inner fluid is soybean oil. $Q_{\mathrm{OF}}/Q_{\mathrm{IF}}$ is 150 (Q_{IF}=6 µl/min). (**f**) Diameter distribution of soybean oil droplets in (**e**). These results show that the AFFD is able to produce both W/O droplets and O/W droplets without any surface modification and the wetting problem do not occur in the AFFD

droplets in hexadecane with Span 80 (2 wt.%) and in corn oil with lecithin (2 wt.%), respectively. The diameter distributions of these droplets are shown in Fig. 5(c) and (d). The coefficient of variations (CVs), defined as the ratio between the standard deviation and the mean, of these droplets in hexadecane and corn oil are 1.44% and 2.87% respectively, indicating that these droplets are mono-disperse; we consider droplets to be monodispersed when CV is less than 5% (Takeuchi et al. 2005). The AFFD is also able to produce O/W droplets; the inner fluid is
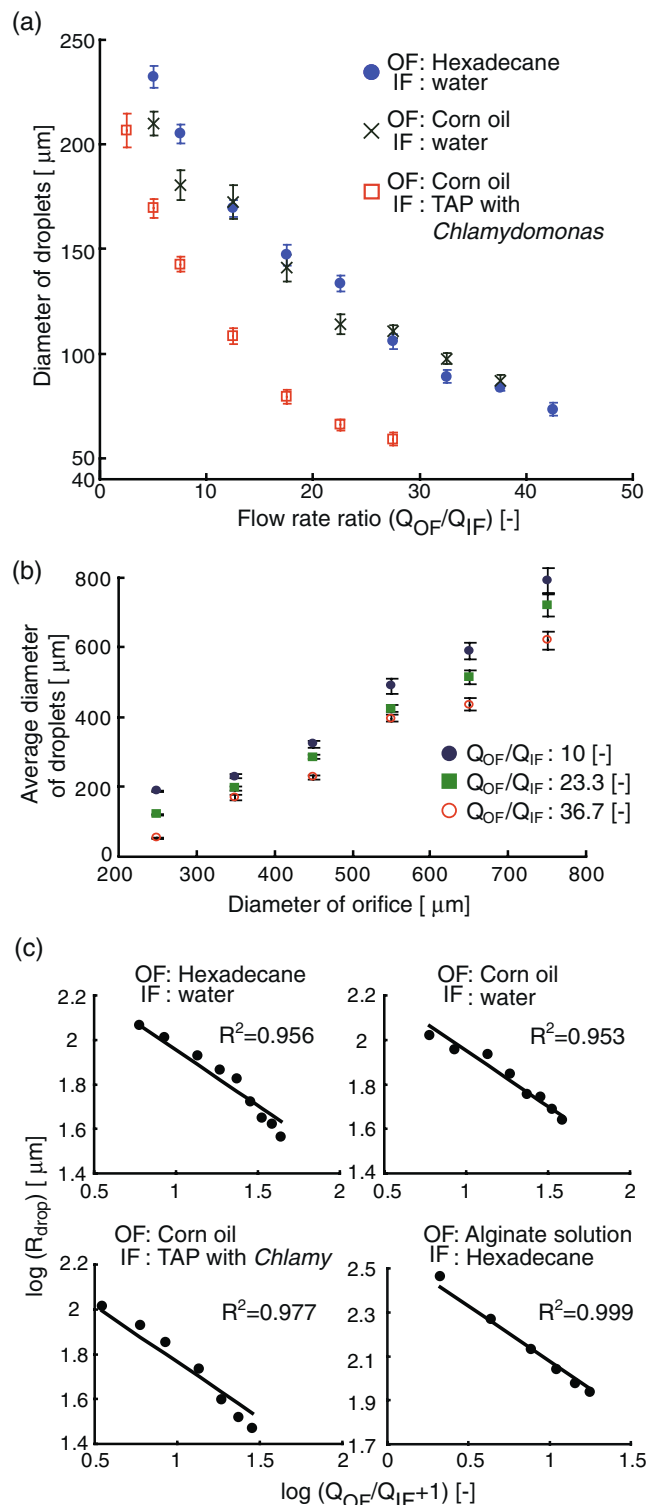
soybean oil and the outer fluid is water with Tween 20 (1.5 wt.%) added as surfactant. Figure 5(e) shows an image of monodisperse O/W droplets and Fig. 5(f) shows the diameter distribution of these droplets. The O/W droplets have an average diameter of 243 μm with a CV of 1.04%. This result indicates that we can avoid the wetting problem in our AFFD as the outer fluid effectively shields the droplets from the channel walls, allowing us to form both W/O and O/W droplets in a single device without the need for surface modifications.

Figure 6(a) illustrates how droplet diameter varies with the flow rate ratio (Q_{OF}/Q_{IF}) for several fluid combinations. Water droplets with diameters ranging from 73.3–244 μm (CV<3.32%) were formed in hexadecane with Span 80 (2 wt.%), and those ranging from 87.2–210 μm (CV< 4.77%) were formed in corn oil with lecithin (2 wt.%). Besides the formation of water droplets in organic phases, we have also successfully encapsulated microbes such as *Chlamydomonas* (diameter≈10 μm) in droplets of TAP buffer which is a cell culture medium for *Chlamydomonas* (Fig. 6(a)). In this case, we obtained droplet sizes ranging from 59.1–207 μm (CV<4.16%). Regardless of the combination of fluids used, the produced W/O droplets exhibited narrow polydispersity and we observed that as the flow rate ratio increased, the diameter of the W/O droplets decreased. Furthermore, droplet sizes gradually came to a constant value as the flow rate ratio increased. This observation is consistent with previous literature (Takeuchi et al. 2005; Huang et al. 2006).

During the formation of the emulsions, we observed that our AFFD produced emulsions without leakage even at high flow rate (1.5 ml/min) due to the seamless geometry of the devices. In addition, when we use the AFFD with a narrower orifice, the diameter of droplets becomes smaller (Fig. 6(b)). The results indicate that monodisperse droplets of varying sizes can be produced by either controlling the flow rate ratio and/or the diameter of the orifice. If smaller droplets are desired, a hybrid method that combines stereolithography with photolithography (Morimoto et al. 2008) can be used to make smaller orifices to produce monodisperse droplets.

We can apply Eq. 5 to all of the W/O droplets in Fig. 6(a) since the capillary numbers at the orifice are below 1 for all these cases. We compared our experimental data to the derived theoretical model (Eq. 5) by plotting a double logarithmic graph shown in Fig. 6(c). From our

Fig. 6 (a) Plot of the size of W/O and O/W droplets produced with the same AFFD versus flow rate ratio (Q_{OF}/Q_{IF}) (Q_{IF}=12 μl/min for all experiments). (CV: min 1.87%–max 3.32% when OF is hexadecane, min 2.72%–max 4.77% when OF is corn oil, min 2.52%–max 4.16% when IF consists of Chlamydomonas.) (b) Plot of the size of W/O droplets formed versus the AFFD's orifice diameter for fixed flow rate ratios (the outer fluid: hexadecane, the inner fluid: water, Q_{IF}=9 μl/min). (c) Experimental data with line (gradient=−0.5) fitted using least squares methods. We can use this fitting line when Ca<1. Ca is computed using the following fluid properties: η_{of}=0.075 Pa·s and γ=0.02 mN/m for corn oil, and η_{of}=0.0033 Pa·s and γ=0.03 mN/m for hexadecane. (In fig. (b), Chlamy is Chlamydomonas and R^2 is coefficient of dimension)
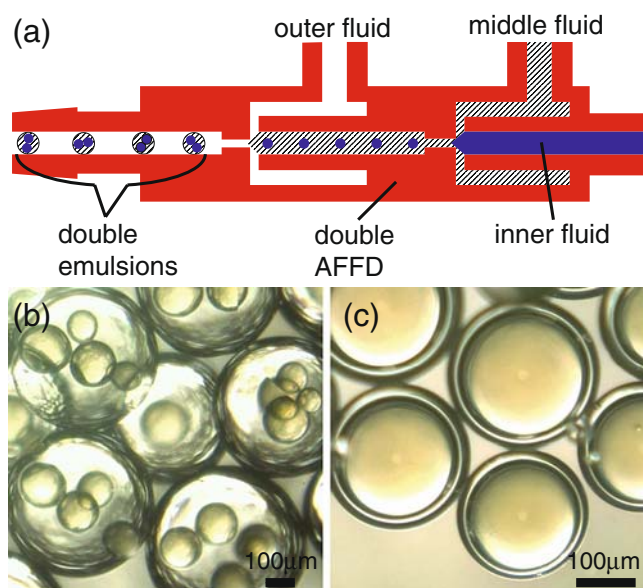
Fig. 7 (**a**) Cross-sectional diagram of the double AFFD using stereolithography to produce double emulsions. The inner fluid is water with 3 wt.% red ink , middle fluid is corn oil with 2 wt.% lecithin and outer fluid is water with 1.5 wt.% Tween 20. (**b**, **c**) Images of double emulsions. (flow rate of the inner fluid (Q_{IF})=6 μl/min, flow rate of the middle fluid (Q_{MF})=120 μl/min, and flow rate of the outer fluid (Q_{OF})=500 μl/min in (**b**). Q_{IF}=12 μl/min, Q_{MF}=150 μl/min, Q_{OF}=500 μl/min in (**c**))

model, $\log(R_{drop})$ is proportional to $-\frac{1}{2}\log\left(\frac{Q_{OF}}{Q_{IF}}+1\right)$. When we fitted the data with lines having gradients of $-\frac{1}{2}$ using the least squares method, the coefficient of determinations obtained were over 0.95 for all the lines, indicating that our experimental data are in good agreement with the theoretical expression. In addition, we fitted the experimental data of O/W droplets with a line by the same method (Fig. 6(c)). We are able to produce the monodisperse O/W droplets (the diameters ranging from 110–196 μm, CV<3.16%) using hexadecane in the inner fluid and sodium alginate solution (3 wt.%) in outer fluid. The coefficient of determination was over 0.99, indicating that they are also in good agreement with the theoretical expression. From this result, we think that the AFFDs can produce O/W droplets in a dripping regime.

3.2 Formation of double emulsions

We used a modified device comprising of two integrated AFFDs (Fig. 7(a)) to demonstrate that beside single emulsions, we can also produce double emulsions without surface modifications. Conventional devices for forming monodisperse double emulsions are complicated and difficult to fabricate, but stereolithography can fabricate double AFFDs automatically and allow us to control their dimensions easily. We succeeded in forming different types

of double emulsions. Figure 7(b) and (c) are images of the double emulsions formed in which the inner fluid is water with red ink (3 wt.%), middle fluid is corn oil with lecithin (2 wt.%) and outer fluid is water with Tween 20 (1.5 wt.%). We believe that AFFDs fabricated using stereolithography can be a convenient platform for the formation of double or even multi-emulsions since (a) stereolithography is able to fabricate an integrated device comprising of multi AFFDs
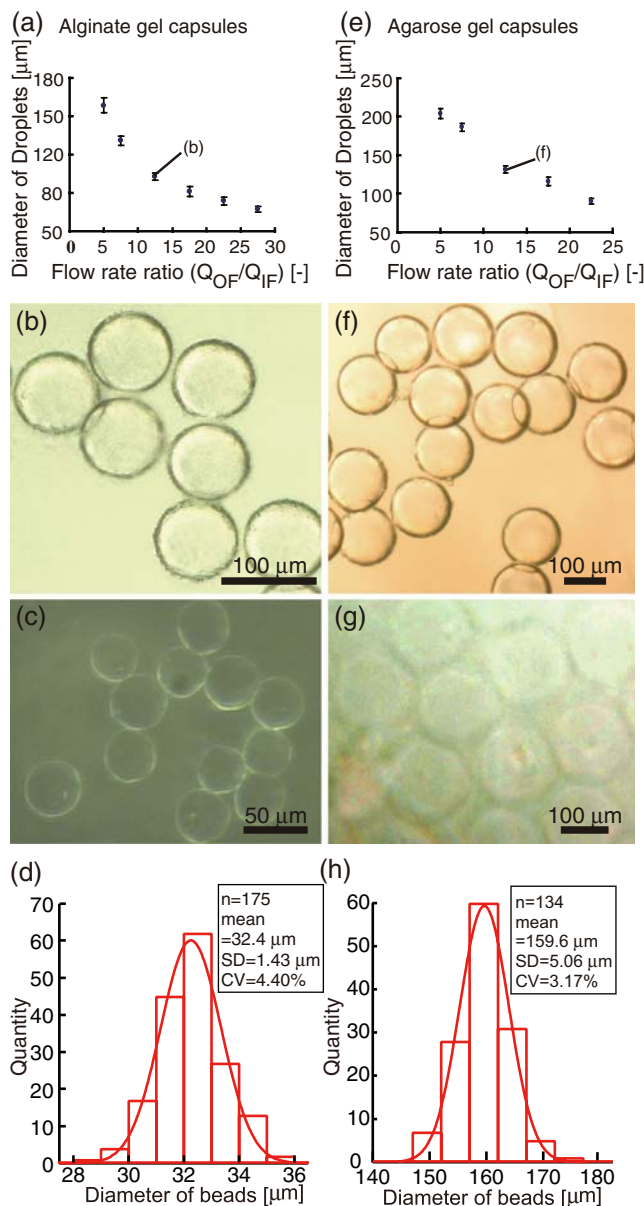

Fig. 8 (**a**) Plot of the size of alginate gel beads in the corn oil versus flow rate ratio (Q_{IF}=12 μl/min for all experiments). (CV: min 2.85%–max 4.63%) (**b**) Image of alginate gel beads in corn oil corresponding to (**b**) in figure (**a**). (**c**) Photo of alginate gel beads in water after rinsing (**b**). (**d**) Diameter distribution of alginate gel beads in water. (**e**)–(**h**) The demonstration of the formation of monodisperse agarose gel beads (CV: min 2.61%–max 4.80%). Graphs and images are in the same sequence as alginate gel beads

with minimal misalignment together with multiple connection ports, and (b) the formation of emulsions in AFFDs does not require any surface modification to the device.

3.3 Formation of monodisperse hydrogel beads

It has been reported that the fouling of channel surfaces by proteins and carbohydrates may make the formation of even W/O dispersions in hydrophobic channels difficult for formation of alginate hydrogel beads (Tan and Takeuchi 2007) and in order to circumvent this problem, it is necessary to modify the surface of 2D microfluidic channels (e.g., silanization) to cater for each usage. Here, we successfully demonstrated the formation of both alginate and agarose gel beads with our device. Figure 8(a) is a plot of the diameter of alginate beads in corn oil as a function of the flow rate ratio. Figure 8(b) shows alginate gel beads in corn oil taken immediately after formation, and Fig. 8(c) shows the same gel beads in water after rinsing with *washing buffer*. Average diameter of alginate gel beads in water (32 μm) was smaller than that in corn oil (81 μm). The final beads were smaller than the droplets produced because alginate gelated over time and rinsing with *washing buffer* that included Ca^{2+} ions caused a further shrinkage (Tan and Takeuchi 2007). The distribution of the diameter of alginate gel beads in water (Fig. 8(d)) indicates that the alginate gel beads kept their monodispersity when we transferred them into water. Similar to alginate gel beads, the diameter of agarose gel beads formed decreased when the flow rate ratio increased (Fig. 8(e)). Figure 8(f) and (g) are images of agarose gel beads in corn oil and those in water after rinsing with Tween 20 solution (1 wt.%), respectively. In contrast to alginate gel beads, these agarose gel beads swelled in water and their diameter (159 μm) in water was larger than that in corn oil (131 μm). Figure 8(h) is a plot showing the diameter distribution of the agarose gel beads in water, which indicates that these gel beads were monodisperse. These images and plots indicate that similar to the formation of W/O droplets, the AFFD is able to produce monodisperse hydrogel beads and vary their size with respect to the flow ratio. The AFFDs allow us to produce monodisperse hydrogel beads regardless of components of hydrogel solutions including cells and/or biological molecules such as deoxyribonucleic acids (DNAs) and proteins that caused the wetting problem in 2D microchannels, which can be used for cell culturing and DNA analysis.

4 Conclusion

Using stereolithography, we designed and fabricated a monolithic AFFD. In our devices, we can produce various kinds of droplets and double emulsions without experiencing any wetting problem and leakage. These samples had CVs of less than 5% and we confirmed that the size of the droplets produced corresponded well with the derived theoretical model. Besides W/O and O/W droplets, we also successfully demonstrated the formation of uniform alginate and agarose gel beads with our device. These hydrogel beads have many potential applications in diverse fields ranging from pharmaceutical to biomedical industries. By modifying the design of the axisymmetric flow-focusing orifice and controlling flow rates of the inner and outer fluids, it will be possible to produce droplets, multi emulsions and hydrogel beads in the order of a few micrometers for applications that require small capsules such as in single cell encapsulation and drug delivery systems. Also, the hybrid methods combined stereolithography and other methods allow AFFDs to incorporate objects such as filters or valves fabricated by other methods during the stereolithography process to have more possibility of applications than conventional ones. We believe that the ease of fabrication and operation of the AFFD will make it an convenient tool for researchers without any experience in microfludics and knowledge of micro-fabrication techniques such as chemists and biologists.

References

B. Ambravaneswaran, H.J. Subramani, S.D. Phillips, O.A. Basaran, Phys. Rev. Lett. **93**, 034501 (2004). doi:10.1103/PhysRevLett.93.034501

S.L. Anna, N. Bontoux, H.A. Stone, Appl. Phys. Lett. **82**, 364 (2003). doi:10.1063/1.1537519

C.H. Choi, J.H. Jung, Y.W. Rhee, D.P. Kim, S.E. Shim, C.S. Lee, Biomed. Microdevices **9**, 855 (2007). doi:10.1007/s10544-007-9098-7

P. Garstecki, I. Gitlin, W. DiLuzio, G.M. Whitesides, E. Kumacheva, H.A. Stone, Appl. Phys. Lett. **85**, 2649 (2004). doi:10.1063/1.1796526

N.B. Graham, M.E. Mcneill, Biomaterials **5**, 27 (1984). doi:10.1016/0142-9612(84)90063-2

S.H. Huang, W.H. Tan, F.G. Tseng, S. Takeuchi, J. Micromech. Microeng **16**, 2336 (2006). doi:10.1088/0960-1317/16/11/013

A.C. Jen, M.C. Wake, A.G. Mikos, Biotechnol. Bioeng. **50**, 357 (1996). doi:10.1002/(SICI)1097-0290(19960520)50:4<357::AID-BIT2>3.0.CO;2-K

J.W. Kim, A.S. Utada, A. Fernandez-Nieves, Z.B. Hu, D.A. Weitz, Angew. Chem. Int. Ed. **46**, 1819 (2007). doi:10.1002/anie.200604206

G. Luca, M. Calvitti, C. Nastruzzi, L. Bilancetti, E. Becchetti, G. Angeletti et al., Tissue Eng. **13**, 641 (2007). doi:10.1089/ten.2006.0137

A. Luque, F.A. Perdigones, J. Esteve, J. Montserrat, A.M. Ganan-Calvo, J.M. Quero, J. Microelectromech. Syst. **16**, 1201 (2007). doi:10.1109/JMEMS.2007.901644

L. Martin-Banderas, A. Rodriguez-Gil, A. Cebolla, S. Chavez, T. Berdun-Alvarez, J.M.F. Garcia, M. Flores-Mosquera, A.M. Ganan-Calvo, Adv. Mater. **18**, 559 (2006). doi:10.1002/adma.200501976

Y. Morimoto, K. Kuribayashi, S. Takeuchi, Proc. MicroTAS 2008 Conference, 2008, 1015 (2008)

T. Nisisako, T. Torii, T. Higuchi, Lab Chip **2**, 24 (2002). doi:10.1039/b108740c

Y.L.M. Nortier, J.A. Vandehaven, C.H.W. Koks, J.H. Beijnen, Pharm. World Sci. **17**, 214 (1995). doi:10.1007/BF01870614

S. Okushima, T. Nisisako, T. Torii, T. Higuchi, Langmuir **20**, 9905 (2004). doi:10.1021/la0480336

D. Poncelet, Ann. N. Y. Acad. Sci. **944**, 74 (2001)

P. Sanguansri, M.A. Augustin, Trends Food Sci. Technol. **17**, 547 (2006). doi:10.1016/j.tifs.2006.04.010

H. Shintaku, T. Kuwabara, S. Kawano, T. Suzuki, I. Kanno, H. Kotera, Microsyst. Technol. **13**, 951 (2007). doi:10.1007/s00542-006-0291-z

S. Sugiura, T. Oda, Y. Izumida, Y. Aoyagi, M. Satake, A. Ochiai et al., Biomaterials **26**, 3327 (2005). doi:10.1016/j.biomaterials.2004.08.029

S. Takeuchi, P. Garstecki, D.B. Weibel, G.M. Whitesides, Adv. Mater. **17**, 1067 (2005). doi:10.1002/adma.200401738

W.H. Tan, S. Takeuchi, Adv. Mater. **19**, 2696 (2007). doi:10.1002/adma.200700433

S. Tomotika, Proc. R. Soc. Lond. A **150**, 322 (1935)

A.S. Utada, E. Lorenceau, D.R. Link, P.D. Kaplan, H.A. Stone, D.A. Weitz, Science **308**, 537 (2005). doi:10.1126/science.1109164

A.S. Utada, L.Y. Chu, A. Fernandez-Nieves, D.R. Link, C. Holtze, D.A. Weitz, MRS Bull. **32**, 702 (2007)

X. Zhang, X.N. Jiang, C. Sun, Sensors Actuators A **77**, 149 (1999). doi:10.1016/S0924-4247(99)00189-2

H. Zhang, E. Tumarkin, R.M.A. Sullan, G.C. Walker, E. Kumacheva, Macromol. Rapid Commun. **28**, 527 (2007). doi:10.1002/marc.200600776

S. Zissi, A. Bertsch, J.Y. Jezequel, S. Corbel, D.J. Lougnot, J.C. Andre, Microsyst. Technol. **2**, 97 (1996). doi:10.1007/BF02447758